FULL PAPER

BJC

British Journal of Cancer (2014) 111, 477–485 | doi: 10.1038/bjc.2014.342

Keywords: angiogenesis; splicing; melanoma

Targeting SRPK1 to control VEGF-mediated tumour angiogenesis in metastatic melanoma

M V Gammons*[,1], R Lucas[1], R Dean[1], S E Coupland[2], S Oltean[1] and D O Bates*[,1,3]

[1]*Microvascular Research Laboratories, School of Physiology and Pharmacology, Preclinical Veterinary Sciences Building, University of Bristol, Southwell Street, Bristol BS2 8EJ, UK;* [2]*Department of Molecular and Clinical Cancer Medicine, University of Liverpool, Liverpool, UK and* [3]*Cancer Biology, Division of Cancer and Stem Cells, School of Medicine, University of Nottingham, Queen's Medical Centre, Nottingham NG2 7UH, UK*

Background: Current therapies for metastatic melanoma are targeted either at cancer mutations driving growth (e.g., vemurafenib) or immune-based therapies (e.g., ipilimumab). Tumour progression also requires angiogenesis, which is regulated by VEGF-A, itself alternatively spliced to form two families of isoforms, pro- and anti-angiogenic. Metastatic melanoma is associated with a splicing switch to pro-angiogenic VEGF-A, previously shown to be regulated by SRSF1 phosphorylation by SRPK1. Here, we show a novel approach to preventing angiogenesis—targeting splicing factor kinases that are highly expressed in melanomas.

Methods: We used RT–PCR, western blotting and immunohistochemistry to investigate SRPK1, SRSF1 and VEGF expression in tumour cells, and *in vivo* xenograft assays to investigate SRPK1 knockdown and inhibition *in vivo*.

Results: In both uveal and cutaneous melanoma cell lines, SRPK1 was highly expressed, and inhibition of SRPK1 by knockdown or with pharmacological inhibitors reduced pro-angiogenic VEGF expression maintaining the production of anti-angiogenic VEGF isoforms. Both pharmacological SRPK1 inhibitors and SRPK1 knockdown reduced growth of human melanomas *in vivo*, but neither affected cell proliferation *in vitro*.

Conclusions: These results suggest that selective blocking of pro-angiogenic isoforms by inhibiting splice-site selection with SRPK1 inhibitors reduces melanoma growth. SRPK1 inhibitors may be used as therapeutic agents.

Cutaneous melanoma (CM) arises from neoplastic melanocytes of the skin (Gray-Schopfer *et al*, 2007), and occurs with a frequency of 13 000 new cases each year in the United Kingdom. Melanoma can occur in other parts of the body, such as the uveal tract (Chang *et al*, 1998) as well as in mucosal (e.g., conjunctiva, rectum and vagina), subungual and acral sites. Uveal melanoma (UM), although rare, is the most common intraocular tumour in adults (Damato, 2012). The major cause of death in CM and UM is dissemination of the primary tumour (Jemal *et al*, 2008). For example, 20% of CM patients present with metastases, with the median 5-year survival of these patients being 5%. Up to 50% of patients with UM will develop metastatic disease, usually to the liver, and this is fatal owing to present ineffective therapies (Damato, 2012). Particular prognostic parameters are known in both CM and UM (Damato *et al*, 2011), however, predictive biomarkers that can foretell response to therapies are of paramount importance.

Sustained angiogenesis, one of the hallmarks of cancer (Hanahan and Weinberg, 2000), is required for the growth and metastasis of primary tumours (Folkman, 1971). VEGF, a critical regulator of both normal and pathological angiogenesis has been the focus of anti-angiogenic targets over the last decade. In patients suffering from CM, an increase in angiogenesis with metastatic potential and disease transition to a more aggressive vertical growth phase has been described (Erhard *et al*, 1997). Furthermore, high levels of numerous cytokines including VEGF have been identified in ocular tumours from patients who develop secondary retinal and iris NV following ionising radiation treatment of their tumours (Boyd *et al*, 2002).

*Correspondence: Dr MV Gammons; E-mail: melissag@mrc-lmb.cam.ac.uk or Professor DO Bates; E-mail: David.Bates@nottingham.ac.uk

Revised 23 April 2014; accepted 1 May 2014; published online 10 July 2014

Current FDA-approved therapies for the treatment of CM metastases following surgery of the primary tumour include the chemotherapeutic agent, dacarbazine, which shows a response rate in 7–12% of patients (Bedikian *et al*, 2006; Chapman *et al*, 2011), vemurafenib specifically for the treatment of melanomas containing the $BRAF^{V600E}$ mutation (Flaherty *et al*, 2011) present in 40–60% of melanomas (Davies *et al*, 2002; Curtin *et al*, 2005); and the CTLA4 antibody ipilimumab (Lipson and Drake, 2011). Chemotherapy and radiation therapy used in CM does not seem to be effective for the treatment of metastatic UM. Currently, there are no FDA-approved VEGF inhibitors for use in metastatic melanoma; however, the anti-VEGF monoclonal antibody, bevacizumab, has been shown to suppress micrometastases in experimental ocular melanoma (Yang *et al*, 2010), and a Phase II clinical trial showed combined treatment of bevacizumab with interferon-α improved disease stabilisation in a quarter of metastatic UM patients (Varker *et al*, 2007). Although VEGF is upregulated in melanoma, its overall expression has been shown to correlate poorly with metastatic spread (Stefanou *et al*, 2004). However, VEGF can be generated as two isoform families, the pro-angiogenic VEGF-A_{xxx} family, and the anti-angiogenic VEGF-A_{xxx}b family, where xxx refers to the number of amino acids in the secreted protein encoded by the spliced mRNA (Harper and Bates, 2008). In 2007, Pritchard-Jones *et al* identified anti-angiogenic $VEGF_{xxx}$b staining in the normal epidermis surrounding human melanomas, but only weak staining in a small proportion of melanoma samples, and observed a decrease in $VEGF_{xxx}$b expression in primary tumours that had gone on to metastasise. VEGF splicing is regulated by the SR protein kinase SRPK1 (Nowak *et al*, 2010), and it has been shown that in a carcinoma cell line (LS174t) the splicing of VEGF can be modulated to prevent the production of pro-angiogenic isoforms through the lentiviral knockdown of SRPK1. Cells with reduced SRPK1 expression levels increased the production of $VEGF_{165}$b and had reduced expression of $VEGF_{165}$, and when these cells were implanted subcutaneously in a xenograft tumour model the cancers grew significantly slower compared with cells expressing a lentiviral control (Amin *et al*, 2011). We, therefore, aimed to investigate the role of SRPK1 regulating VEGF isoform expression in cutaneous and UM cell lines.

MATERIALS AND METHODS

Cell culture and transfection. CM cell line, A375 (ATCC, Middlesex, UK), and UM cell lines, 92.1, Mel270 and Omm2.5 cells were cultured in DMEM, 10% FBS, 0.5% PenStrep and split at 80% confluence. A375 melanoma cells were treated with culture medium plus 6 μg polybrene and 1 μl scrambled shRNA ($T = 2.25 \times 10^4$) or 5 μl SRPK1 shRNA ($T = 3.44 \times 10^8$; SMART Vector 2.0, Dharmacon, Thermo Scientific, Lafayette, LA, USA) per 200 000 cells. Cells transduced with the lentivirus were selected using puromycin at 2 μg ml^{-1}. Transduction efficiency was determined by green fluorescent protein (GFP) expression.

Pharmacological inhibitor treatments. SRPIN340 (*N*-[2-(1-piperidinyl)-5-(trifluoromethyl)phenyl] isonicotinamide), was purchased from Ascent Scientific, Bristol, UK. Cells at ~70% confluence were serum starved for at least 12 h and treated with 1–10 μM SRPIN340, 0.02–0.05% DMSO was added to vehicle control. After 24 h, mRNA was extracted or cells were fixed for staining, 48 h later protein was extracted, for further analysis.

Cell viability assays. Cell proliferation was determined by two methods. Thirty thousand A375 cells per well, transduced with scrambled shRNA, SRPK1 shRNA or untransduced and treated with SRPIN340, were seeded on 24-well plates. Every 24 h cells were trypsinised and a cell count was performed. Cells seeded on cover slips were also stained for Ki67. For scratch assays, cells were grown to confluence in 24-well plates and a 1-mm-thick line of cells was scratched off the plate along the central line of the well. Each well was imaged at time zero, after 12 h and after 24 h. The percentage of coverage across the scratch was determined (ImageJ, NIH, Bethesda, MD, USA) as a measure of percentage wound closure.

Semi-quantitative PCR and qPCR. Conventional PCR was used to detect $VEGF_{165}$ mRNA. Five percent of the cDNA was added to a reaction mixture containing: 2 × PCR Master Mix (Promega, Southampton, UK), primers (1 μM each) complementary to exon7b (5′-GGCAGCTTGAGTTAAACGAAC-3′) and the 3′-UTR of VEGF (5′-ATGGATCCGTATCAGTCTTTCCTGG-3′) and DNase-/RNase-free water. All samples were run in parallel with negative controls (water and cDNA without reverse transcriptase (-RT)). The reaction mixture was thermocycled (PCR Express, Thermo Electron Corporation, Basingstoke, UK) 30–35 times, denaturing at 95 °C for 60 s, annealing at 55 °C for 60 s and extending at 72 °C for 60 s. PCR products were separated on 2.5% agarose gels containing 0.5 μg ml^{-1} ethidium bromide (Bio-Rad, Hertfordshire, UK) and visualised under an ultraviolet transilluminator (Bio-Rad). Equal cDNA loading was determined by PCR with GAPDH primers (forward: 5′-CACCCACTCCTCCACCTT TGAC-3′; reverse: 5′-GTCCACCACCCTGTTGCTGTAG-3′). Primers result in one amplicon at ~112 bp after thermocycling 30 times, denaturing at 94 °C for 45 s, annealing at 65 °C for 45 s and extending at 72 °C for 60 s. The qPCR reaction was set up using Roche SyBr Green and run in an ABI 7000 (Roche, Burgess Hill, UK). Validated primers specific to SRPK1, 18S ribosomal and GAPDH were used for the qPCR. The reaction was thermocycled 45 times (95 °C for 30 s, 55 °C for 30 s and 72 °C for 60 s).

PanVEGF and $VEGF_{xxx}$b enzyme-linked immunosorbent assay (ELISA). PanVEGF capture antibody (1 μg ml^{-1}) (Duoset VEGF ELISA DY-293; R&D Systems, Minneapolis, MN, USA) was incubated overnight at room temperature. The plates were blocked (Superblock; Thermo Scientific) and serial dilutions of recombinant human (rh)$VEGF_{165}$ or rh$VEGF_{165}$b standards (ranging from 4 ng ml^{-1} to 16.25 pg ml^{-1}) were added, incubated alongside sample lysates, typically diluted 1 : 10. The plate was incubated for 1 h at 37 °C with shaking, washed and incubated with 100 μl per well of either biotinylated goat anti-human VEGF (0.1 μg ml^{-1}; R&D Systems) or mouse anti-human $VEGF_{165}$b (0.25 μg ml^{-1}) for a further 1 h at 37 °C. After washing, 100 μl per well of horseradish peroxidase (HRP)-conjugated streptavidin (1 : 200; R&D Systems) was added and plates were left at room temperature for 20 min.

The plates were washed and colour change was induced with substrate A and B (DY-999; R&D Systems) for 20 min under light protection. The reaction was stopped by addition of 100 μl per well of 1 M H_2SO_4 and the absorbance was read immediately in an ELISA plate reader (Dynex Technologies Opsys MR system plate reader) at 450 nm with a control reading at 570 nm. Revelation Quicklink 4.25 software (Dynex Technologies, Chantilly, VA, USA) was also used to calculate a standard curve from mean absorbance values of standards enabling the estimation of VEGF concentration for each sample.

Western blotting. Protein samples (30–50μg) were mixed with 1 × SDS loading buffer (100 mM Tris-HCl, 4% SDS, 20% glycerol, 0.2% (w/v) bromophenol blue and 5% final concentration 2-mercaptoethanol, pH 6.8). To denature the protein, samples were boiled for 5 min at 100 °C.

Samples were subjected to polyacrylamide gel electrophoresis (PAGE) on a 12% SDS–PAGE gel at 90 V in ice cold running buffer (25 mM Tris-HCl, 250 mM glycine and 0.1% SDS, pH 8.3) for ~2.5 h. The separated proteins were then electrophoretically blotted to a methanol-activated polyvinylidene fluoride membrane (Fisher Scientific, Pittsburgh, PA, USA) by wet transfer for 2 h at 90 V in transfer buffer (50 mM Tris-HCl, 38 mM glycine and 20% methanol, pH 8.3). Membranes were incubated in blocking solution

(2.5% non-fat dried milk in PBS/T or 5% BSA) with agitation at room temperature for 30 min and then probed with the primary antibody overnight at 4 °C; rabbit polyclonal anti-VEGF-A (A20; sc-152, Santa Cruz, Dallas, TX, USA) diluted 1 : 1000-1 : 100 in 2.5% non-fat dried milk TBS-T, $VEGF_{xxx}$b-specific mouse monoclonal 56/1 (R&D Systems) diluted 1 : 1000-1 : 500 in 5% BSA TBS-T, media from mouse hybridoma cell line, mab104 diluted 1 : 4 in TBS-T and goat polyclonal beta-tubulin (Abcam, Cambridge, UK) diluted 1 : 1000 in 5% BSA TBS-T. Membranes were then washed four times for 10 min each with TBS-0.3%T before incubation with secondary HRP-conjugated antibodies: goatαmouse immunoglobulin G (IgG), goatαrabbit IgG or rabbitαgoat IgG (Pierce, Rockford, IL, USA) diluted 1 : 10 000 in 5% BSA TBS-T or 2.5% non-fat dried milk TBS-T, for 45 min at room temperature with agitation. The washes were repeated and the bands were detected using the Enhanced Chemoluminiscence (ECL) SuperSignal West Femto Maximum Sensitivity Substrate kit (Pierce).

Immunofluorescence staining and imaging. For immunofluorescence, cells were grown to 80% confluence on glass cover slips. After treatment the cells were washed with PBS, fixed for 5 min with 4% PFA and then washed with PBS in 0.05% Triton X (PBS-TritonX). The cells were blocked in 5% normal goat serum in PBS-TritonX for 1 h, washed thrice with PBS-TritonX and incubated overnight with 2 $\mu g\,ml^{-1}$ of mouse monoclonal SRSF1 (96; sc-33652, Santa Cruz) or 2 $mg\,ml^{-1}$ mouse monoclonal anti-SRPK1 (BD Biosciences, Franklin Lakes, NJ, USA, 611072). The cells were washed thrice with PBS-Triton and incubated with goat anti-mouse Alexa Fluor 555 diluted 1 : 100 in 1 × PBS for visualisation and counterstained for the nucleus with Hoescht. Images were taken at × 40 objective using a microscope (Nikon Eclipse E400, Nikon, Surrey, UK).

CD31 Immunohistochemistry. Serial 7-μm sections of PFA-fixed paraffin wax-embedded tumour parts were mounted onto slides. Vessel presence was confirmed by CD31 staining. Sections were blocked in 5% normal goat serum for 30 min, CD31 antibody (Abcam 805662; diluted 1 : 50) was added overnight, 2 $\mu g\,ml^{-1}$ anti-rabbit biotin antibody (Vector Laboratories, Burlingame, CA, USA) for 1 h followed by the avidin–biotinylated enzyme complex (ABC, Vector Laboratories) for 30 min followed by the DAB substrate (Vector Laboratories). Sections were co-stained with haematoxylin and examined using a Nikon Eclipse E400 microscope, and photos were captured using Nikon Eclipse Net software (Nikon Instruments, Melville, NY, USA).

***In vivo* tumour model.** All animal experiments were carried out under a UK Home Office License after approval by the University of Bristol Ethical Review Group. A375, A375 shRNA control and A375 shRNA SRPK1 knockdown cells were cultured in T75 flasks to 80% confluence. Trypsinised cells were counted using a haemocytometer, and 2 million cells of A375 shRNA control and A375 shRNA SRPK1 were injected subcutaneously either into the left and right flanks of nude mice, or a single injection of untransduced A375 cells. Tumour-bearing mice (> 3 mm) were weighed and tumours were measured by caliper bi-weekly. Mice bearing A375-untransfected tumours were treated with either 100 μl of 20 $\mu g\,ml^{-1}$ SRPIN340 (diluted 100 × in PBS from 2 $mg\,ml^{-1}$ stock in DMSO), or 100 μl of 1% DMSO vehicle control injected daily into the peritumoral space. Tumour volumes were calculated according to the formula $(A \times B \times (A+B)/2)$ where A = length of the tumour and B = tumour width. The mice were culled by cervical dislocation (according to Schedule 1 under the Animal (Scientific Procedures) Act 1986), when the first tumour in each experimental groups reached 16 mm maximum length. The tumours were excised, weighed and either stored in 4% PFA diluted in 1 × PBS or frozen down to − 80 °C for further analysis. Investigators were blinded to each group when performing injections, taking measurements and analysing data.

Statistical analysis. Data are shown as mean ± s.e.m. All data, graphs and statistical analyses were calculated with Microsoft Excel (Microsoft Office Software, Reading, UK), GraphPad Prism (GraphPad Software Inc., La Jolla, CA, USA) and ImageJ. All results were considered statistically significant at $^{*}P<0.05$, $^{**}P<0.01$ and $^{***}P<0.001$.

RESULTS

SRPK1 acts through SRSF1 to regulate pro-angiogenic VEGF expression in melanoma cells. To determine the expression of SRPK1 in different melanoma cell lines, mRNA extracted from CM and UM cell lines was assayed by qRT–PCR and compared with primary pigmented epithelial cells (retinal-pigmented epithelial cells-RPE). All melanoma cell lines expressed significantly more SRPK1 than primary RPE cells with A375 expressing significantly more than UM cell lines, which expressed between 20 and 50% of the levels found in A375 cells relative to internal controls (Mel270, 48 ± 6%; 92.1, 34 ± 7%; Omm2.5, 21 ± 51%; Figure 1A).

At the protein level, SRPK1 and SRSF1 was expressed in all melanoma cell lines with higher expression levels of SRPK1, and possibly SRSF1 appearing in metastatic cell lines, A375 and Omm2.5 (Figure 1B) than in Mel270 and 92.1. A similar relative expression of $VEGF_{165}$ expression at the RNA level was seen (i.e., expression in A375 and Omm2.5, but not Mel270 or 92.1 Figure 1C) and total (pan) VEGF was higher in A375, Omm2.5 and Mel270 than 92.1, whereas the anti-angiogenic $VEGF_{xxx}$b isoforms appeared stronger in the primary (Mel270 and 92.1) compared with metastatic cell lines. (Figure 1D), suggesting that the pro-angiogenic isoforms were raised in metastatic cell lines (Omm2.5 and A375) relative to Mel270 and 92.1.

SRPK1 has been inextricably linked to the phosphorylation of the splicing factor SRSF1 (Ghosh and Adams, 2011). Inhibition of SRPK1 by SRPIN340 prevents the nuclear localisation of SRSF1 induced by IGF-1 in podocytes (Nowak *et al*, 2010) and EGF induced SR-protein phosphorylation in ARPE-19 cells (Gammons *et al*, 2013). Thus, serum-starved A375, Omm2.5, Mel270 and 92.1 cells were treated with 100 nM IGF-1 both alone and in the presence of 10 μM SRPIN340 or left untreated. Twenty-four hours after treatment, cells were stained for SRSF1 (Figure 2A) or SRPK1 (Figure 2B) and nuclei co-stained for Hoescht. In A375 cells IGF-1 induced a significant increase in the percentage of nuclear SRSF1 compared with untreated ($P<0.05$ one-way ANOVA Bonferonni *post hoc*). When IGF-1 treatment was combined with SRPIN340, there was a 54% reduction in the IGF-1 induced nuclear localisation of SRSF1 compared with untreated cells (although this did not reach statistical significance). In UM cell lines a variable response to treatment was observed. In Mel270, IGF-1 increased nuclear localisation of SRSF1 compared with untreated cells, and SRPIN340 significantly reduced the proportion of nuclear SRSF1 compared with IGF-1 treatment alone ($P=0.018$). However, in Omm2.5 and 92.1 UM cells no effect of IGF-1 treatment on SRSF1 staining in the nucleus was observed and accordingly no effect of combined SRPIN340 treatment was seen. In all three UM cell lines, nuclear SRPK1 increased and this translocation was unaffected by SRPIN340 treatment (Figure 2B). We further determined the effect of VEGF expression following SRPK1 inhibition. SRPIN340 reduced $VEGF_{165}$ mRNA in a dose-dependent manner in all four cell lines tested (Figure 2C). Furthermore, total VEGF protein was similarly reduced by SRPIN340 reaching significance at 10 μM in A375, Omm2.5 and 92.1 cells (Figure 2D). Anti-angiogenic isoforms were not detected above background levels in these samples.

SRPK1 knockdown reduces pro-angiogenic VEGF and tumour growth *in vivo*. To confirm that VEGF levels can be regulated by

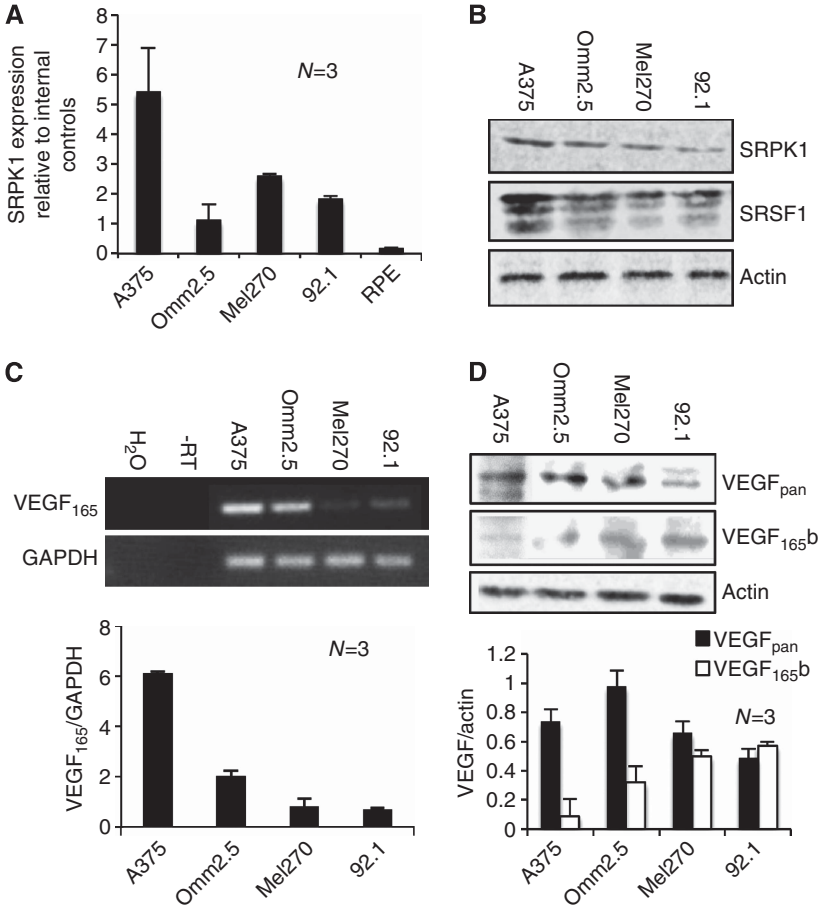

Figure 1. SRPK1, SRSF1 and VEGF expression in cutaneous and uveal melanoma cell lines. (**A**) SRPK1 mRNA expression was greater in melanoma cell lines compared with primary RPE cells. (**B**) SRPK1 and SRSF1 protein expression was stronger in metastatic cell lines, A375 and Omm2.5, and this correlated with greater $VEGF_{165}$ mRNA (**C**) and panVEGF protein expression (**D**). $VEGF_{xxx}b$ protein conversely, appeared stronger in primary cell lines Mel270 and 92.1. Experiments were performed in triplicate.

SRPK1, a lentiviral approach to knock down SRPK1 expression levels was used in the CM cell line A375. A375 cells had previously shown high endogenous SRPK1 expression. Cells were transduced with shRNA control or shRNA SRPK1 and selected with puromycin confirmed by GFP expression (Figure 3A). Knockdown was confirmed at the protein (Figure 3B) and RNA levels (Figure 3C) by western blot and qRT–PCR, respectively. Initially, we investigated the effect of SRPK1 knockdown on SRSF1 nuclear localisation as a measure of phosphorylation. We observed predominantly nuclear staining and the immunofluorescent signal was reduced in SRPK1 knockdown cells (Figure 3D). The reduction in SRSF1 protein expression by SRPK1 shRNA was confirmed by western blotting ($P<0.05$; Figure 3E). SRPK1 knockdown did not affect the level of SRSF1 mRNA, suggesting a potential role for SRPK1 in partially regulating SRSF1 stability. We further investigated SRSF1 siRNA on VEGF expression and saw a reduction in total VEGF expression by western blotting; however, $VEGF_{xxx}b$ isoform expression was unchanged, suggesting, consistent with the hypothesis, that SRPK1 and its substrate SRSF1 act to reduce pro-angiogenic VEGF expression (Figure 3F). The effect of SRPK1 knockdown upon $VEGF_{165}$ mRNA was similar to the effect of SRPIN340 treatment—shRNA SRPK1 significantly reduced $VEGF_{165}$ expression compared with shRNA control-transduced cells ($P<0.01$, Student's *t*-test; Figure 3G). We confirmed this effect at protein level observing not only a significant reduction in pro-angiogenic VEGF, but additionally a significant increase in anti-angiogenic isoforms (Figure 3H).

Before *in vivo* assessment, cell proliferation and migration was compared in A375 shRNA control cells *vs* A375 shRNA SRPK1-transduced cells. Importantly, we did not observe any significant difference in either the number of cells (Figure 4A) migration (Figure 4B) or in the percent of proliferating cells (Ki67 + ve, figure 4C). Control and knockdown cells (2×10^6) were subsequently injected subcutaneously into nude mice onto the left and right flanks, respectively. A375 shRNA SRPK1 tumours grew significantly slower than controls ($P<0.001$; two-way ANOVA with repeated measures; Figure 4D). Subsequent analysis on the excised melanoma confirmed lower SRPK1 mRNA expression levels in knockdown tumours and revealed a positive correlation between tumour volume and SRPK1 expression (Figure 4E). Furthermore, the VEGF protein was reduced in knockdown tumours compared with controls but anti-angiogenic $VEGF_{xxx}b$ isoforms were unchanged (Figure 4F).

Administration of SRPIN340 reduces pro-angiogenic VEGF and tumour growth *in vivo*. Similar to SRPK1 knockdown, we saw no alteration in proliferation (Figure 5A) or migration (Figure 5B) of A375 cells when dose dependently treated with SRPIN340. To determine whether SRPIN340 could be used to inhibit tumour growth, we wished to test it *in vivo*. SRPIN340 dissolved in propylene glycol (80%) and DMSO (20%) (but not 20% DMSO/80% water) at 30 mg ml^{-1}. This was administered in a single 100 μl dose (100 mg kg^{-1}) by oval gavage, and blood and tissues sampled and analysed by mass spectrometry. In plasma, SRPIN340 was detected at 1.55 ± 0.91 μg ml^{-1} after 1 h and this decreased to 0.43 ± 0.19 and 0.77 ± 0.2 μg ml^{-1} at 4 and 8 h, respectively. By 24 h the plasma concentration of SRPIN340 was 0.2 ± 0.06 μg ml^{-1}. One phase exponential decay curve fitting

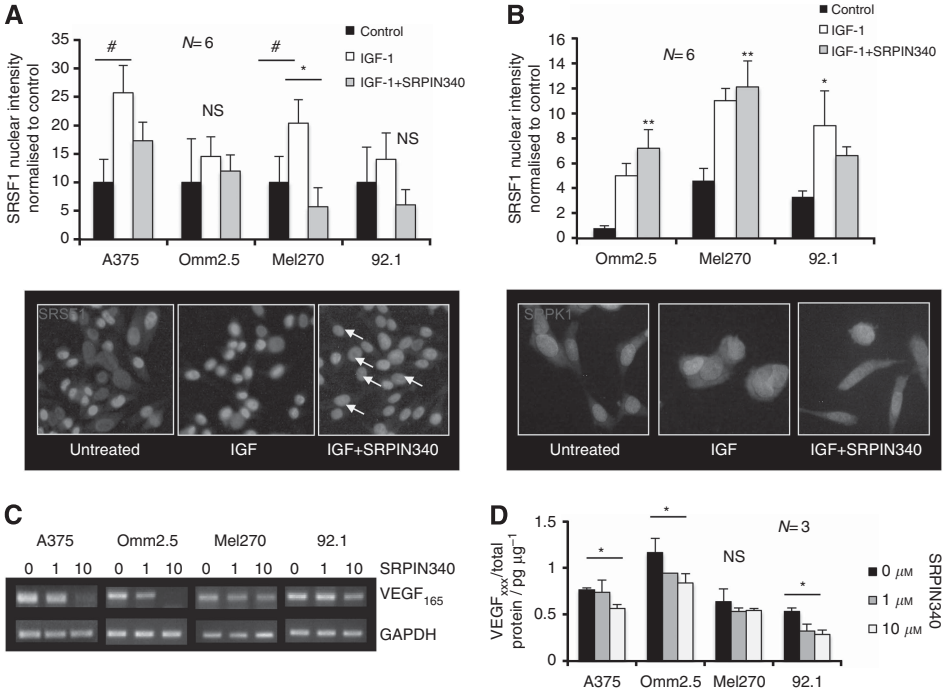

Figure 2. SRPK1 regulates pro-angiogenic VEGF expression in melanoma cells. Serum-starved A375, Omm2.5, Mel270 and 92.1 cells, treated with 5 μM SRPIN340 before IGF-1 administration (100 nM) were stained for (**A**) SRSF1 (red) or (**B**) SRPK1 (red) and co-stained for Hoechst (blue). (**A**) The majority of SRSF1 staining observed was nuclear, but an increase in nuclear intensity following IGF-1 treatment was observed in A375 and Mel270 cells. Pretreatment with SRPIN340 prevented the IGF-1-induced increase in SRSF1 nuclear intensity in Mel270 cells only. $^{\#}P<0.05$. (**B**) SRPK1 staining was mainly cytoplasmic but nuclear intensity was increased following IGF-1 treatment; SRPIN340 was unable to reverse this response. Scale bar, 10 μm. $^{**}P<0.01$. (**C**) Twenty-four hours after inhibitor treatment (1–10 μM) RNA was extracted and cDNA was made for PCR. Treatment with SRPIN340 reduced the expression of $VEGF_{165}$ relative to GAPDH control in all tested cell lines. Water (W) and sample without reverse transcriptase (–RT) were used as negative controls. (**D**) Forty-eight hours after treatment, protein was extracted and assayed for total VEGF and $VEGF_{xxx}b$ by ELISA. The expression of pro-angiogenic VEGF ($VEGF_{xxx}$) was reduced following 10 μM SRPIN340 in A375, Omm2.5 and 92.1 cells (one-way ANOVA, Bonferroni *post hoc*. $^{*}P<0.05$). Arrows show non-nuclear-stained cells. NS, not significant. The full colour version of this figure is available at *British Journal of Cancer* online.

was performed and the sustained half-life of SRPIN340 in plasma (curve fitted from 1 h onwards) was 13.49 h. However, of the 3 mg of SRPIN delivered, total plasma SRPIN340 was estimated at 2.0 μg (30 g mice, 45% haematocrit, 80 ml kg^{-1} blood volume), whereas the concentration in the stomach was 100 $\mu g\,ml^{-1}$ suggesting poor absorption of the drug (Supplementary Figure 1). Furthermore, high DMSO (20%) concentrations would have been required for systemic administration. We thus tried local injection of SRPIN340 *in vivo* to avoid systemic treatment. Untransduced A375 cells were injected subcutaneously and allowed to form tumours. Daily subcutaneous injection of 2 μg SRPIN340 in 100 μl 1 × PBS close to the tumour site significantly reduced tumour growth compared with DMSO (1%) control-injected tumours ($P<0.001$; one-way ANOVA Bonferroni *post hoc*; Figure 5C). Post-tumoral analysis showed reduced total VEGF expression in SRPIN340-treated tumours ($P<0.05$, Student's unpaired *t*-test) and no difference in detection of anti-angiogenic $VEGF_{xxx}b$ isoforms, which did not appear to be affected by treatment (Figure 5D). In this study, unlike the knockdown, tumours were of sufficient size to section and stain for CD31 as a measure of microvascular density (MVD). SRPIN340 significantly reduced MVD compared with vehicle-treated tumours (Figure 5E).

DISCUSSION

We have identified SRPK1 expression in both cutaneous and UM cell lines, and have noted greater expression of both SRPK1 and its main substrate SRSF1 in metastatic compared with primary cell lines (Figure 1). SRPK1 upregulation has been identified in other cancers too, including colon, breast and pancreatic cancers (Hayes *et al*, 2007), glioma (Wu *et al*, 2013) and non-small cell lung carcinoma (Gout *et al*, 2012). SRPK1 overexpression has been identified in Ab subgroups of luminal A breast cancers, the subgroup associated with poor patient prognosis (Finetti *et al*, 2008). Furthermore, in a recent study investigating colon cancer, SRPK1 was upregulated both in adenoma and carcinoma samples (Thorsen *et al*, 2011).

The interaction between SRPK1 and SRSF1 has been well documented; SRPK1 phosphorylates SRSF1 enabling its nuclear localisation and interaction with cellular pre-mRNA (Ghosh and Adams, 2011). The effect of SRPK1 inhibition (using SRPIN340) on SRSF1 subcellular position was examined following induction of SRSF1 translocation to the nucleus using IGF-1 (Nowak *et al*, 2010). IGF-1 appeared to induce nuclear translocation in A375 and Mel270 cells only, and SRPIN340 was only able to block this response in Mel270 cells (Figure 2A). Unlike podocytes (Amin *et al*, 2011), the majority of SRSF1 is nuclear in melanoma cells and thus small changes in the cytoplasmic expression of SRSF1 have been difficult to quantify by this method. What was clear, however, was the effect of SRPK1 inhibition on reducing splicing to the $VEGF_{165}$ isoforms in melanoma cells. SRPIN340 dose dependently reduced $VEGF_{165}$ in all tested cell lines, similar to the effect of SRPIN340 treatment reported in ARPE-19 cells (Gammons *et al*, 2013). In our CM cell line, we were previously unable to consistently determine $VEGF_{165}b$ mRNA expression (Bates *et al*, 2013), possibly owing to high $VEGF_{165}$ levels in melanoma cells competitively inhibiting the detection of $VEGF_{165}b$ (Bates *et al*, 2013), thus only $VEGF_{165}$ was quantified. At the protein level, total

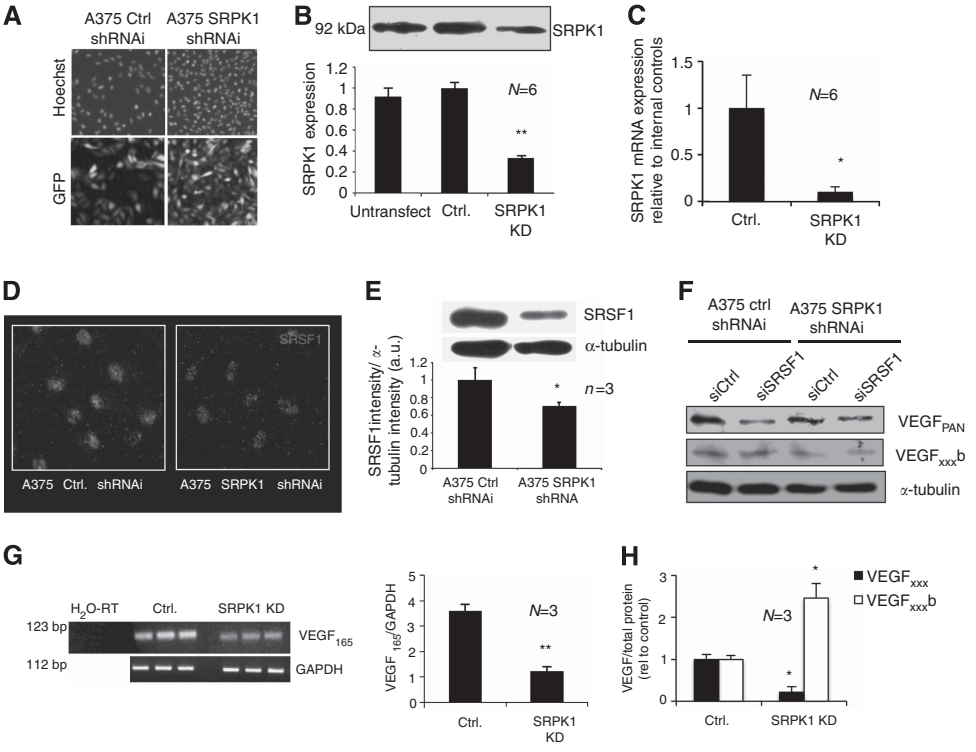

Figure 3. SRPK1 knockdown switches splicing away from pro-angiogenic VEGF. A375 cells were transduced with a lentivirus containing SRPK1 shRNA or scrambled shRNA. (**A**) Transduction efficiency was determined by GFP expression. (**B**) Protein was extracted from cells and tested for SRPK1 expression by immunoblotting. There was a significant reduction in SRPK1 expression after lentiviral shRNA SRPK1 transduction relative to tubulin (**$P<0.01$, one-way ANOVA, Bonferroni *post hoc*). (**C**) SRPK1 mRNA expression in A375 melanoma cells was determined by qPCR and expressed relative to internal control (18S ribosomal). SRPK1 was successfully knocked down in SRPK1 shRNA-transduced cells compared with control cells (*$P<0.05$). (**D**) Staining for SRSF1 confirmed a knockdown in SRPK1 shRNA cells; cell were imaged and images were processed identically (*$P<0.05$, Student's *t*-test). Scale bar, 10 μm. (**E**) Extracted protein was run on an SDS–PAGE and membranes blotted for SRSF1. SRPK1 knockdown weakly knocks down SRSF1 compared with A375 shRNA scramble relative to α-tubulin expression (17%, $n=3$). (**F**) SRSF1 knockdown by siRNA was performed in both control and SRPK1 knockdown cells. SRSF1 siRNA reduced panVEGF without affecting $VEGF_{xxx}b$ expression. (**G**) RT–PCR with primers spanning VEGF exon 7 and the VEGF 3′-UTR were used to determine expression level. SRPK1 knockdown compared with control cells (scrambled shRNA) showed a significant decrease in $VEGF_{165}$ relative to GAPDH ($P<0.01$). (**H**) Extracted protein was assessed by ELISA. In SRPK1 knockdown cells, pro-angiogenic VEGF was significantly decreased ($P<0.05$), whereas $VEGF_{xxx}b$ was significantly upregulated ($P<0.05$).

VEGF was also reduced following SRPIN340 treatment (10 μM) in A375, Omm2.5 and 92.1 cells (Figure 2C).

To confirm the results with targeted genetic inhibition, a lentiviral shRNAi vector transduction approach was used. Both SRPK1 and SRSF1 protein expression was reduced in knockdown cells, confirmed by immunofluorescence, showing a reduction in the intensity of SRSF1 staining. SRPK1 may act in part to regulate the expression of SRSF1 by impacting SRSF1 transcription or translation, although we failed to see a significant change in SRSF1 mRNA levels following SRPK1 knockdown (unpublished data). It was noted in our initial studies that cell lines expressing increased SRPK1 also appeared to express higher SRSF1 levels, which would support an additional level of regulation by the phosphorylating kinase. SRSF1 expression is essential, and depletion of SRSF1 has been reported to cause cell cycle arrest, genomic instability and apoptosis (Li *et al*, 2005). Recent studies have shown SRSF1 negatively autoregulates itself through various post-transcriptional and post-translational mechanisms (Sun *et al*, 2010). The potent oncogenic transcription factor myc (c-myc) has been identified as a factor regulating SRSF1 expression, at least in lung cancer (Das *et al*, 2012). In 2011, Thorsen *et al* showed that active *Wnt* signalling increased the expression of cell-cycle regulator MYC and increased the expression of SRPK1. Taken together, SRPK1 may mediate MYCs control of SRSF1 expression, or may act independently as a partial regulator.

SRSF1 has been shown to regulate the AS of multiple genomic targets (Karni *et al*, 2007; Amin *et al*, 2011). In this study, we observed reduced expression of $VEGF_{165}$ in SRPK1 knockdown cells relative to GAPDH and compared with shRNA control cells ($P<0.01$). This effect on the pre-mRNA splicing was confirmed by assessing protein isoform expression using $VEGF_{xxx}b$-specific and panVEGF ELISAs. There was a significant increase in the expression of $VEGF_{xxx}b$ isoforms (which was clearly detectable above background), and a reduction in $VEGF_{xxx}$ isoforms relative to total VEGF in the SRPK1 knockdown cells relative to control ($P<0.05$, respectively; Figure 3H). Furthermore, SRSF1 siRNA also reduced VEGF expression, similar to the effect of SRPK1 knockdown (Figure 3F).

SRPK1 lentiviral knockdown was not lethal to A375 cells and did not appear to affect cell morphology. Furthermore, proliferation was unaffected by SRPK1 knockdown, and a cell-based scratch assay showed no difference in cell–matrix and cell–cell interactions during cell migration (Figure 4A and B). Although we did not observe significant effects of SRPK1 knockdown *in vitro*, previous studies have identified SRPK1 as a mediator of tumour cell proliferation by acting through MAPK and Akt (also known as protein kinase-B (Hayes *et al*, 2006)). Akt is known for its role in cell migration, and the signalling pathway Akt-SRPK-pSR has been suggested as being involved in cell migration (Zhou *et al*, 2012). As SRPK1 knockdown appeared to reduce the expression of pro-angiogenic VEGF isoforms, isoforms that are necessary for tumour progression, the effect of SRPK1 knockdown on A375 tumour growth *in vivo* was investigated. A375 shRNA SRPK1 tumour grew significantly slower than A375 shRNA control tumours, SRPK1 expression was reduced

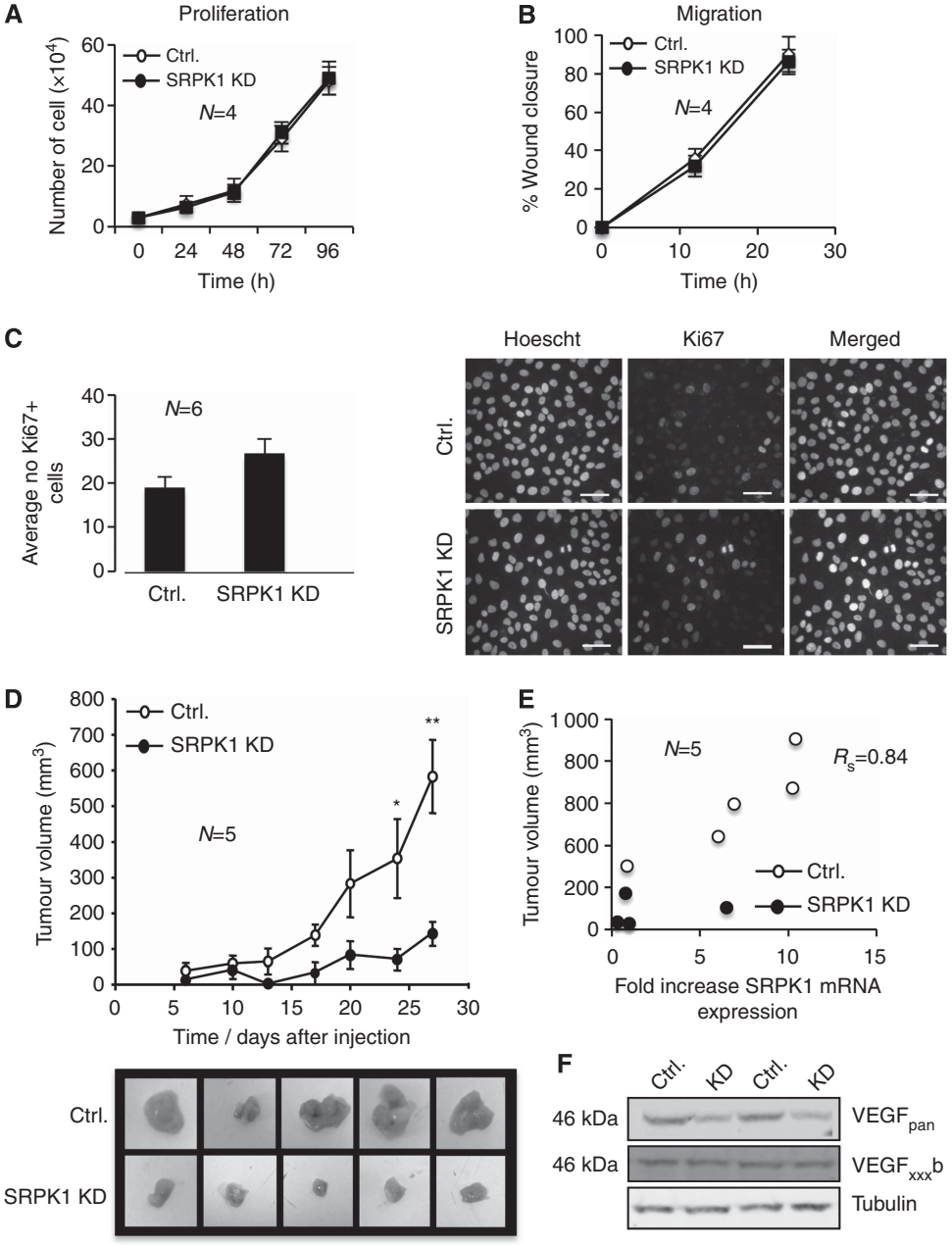

Figure 4. SRPK1 Knockdown is anti-angiogenic and blocks tumour growth. (**A**) A375 control shRNA and A375 SRPK1 shRNA cells were seeded and cells were counted every 24 h for 4 days. There was no difference in proliferation rate between the two cell lines as measured by this method. (**B**) Wells were imaged at time 0 after a 1-mm scratch was performed across the centre of the well, and at 12 and 24 h later. The % coverage of the scratch was calculated. No statistical difference between the coverage of the two cell lines was observed. (**C**) Cells were then fixed and stained for Ki67, an endogenous proliferation marker. Representative images of staining are shown. Cell counts showed no significant difference in the average number of proliferating cells. Scale bar, 10 μm. (**D**) Control and SRPK1 KD cells were injected subcutaneously (2×10^6) into the left and right flanks of nude mice, respectively. Tumour growth was measured bi-weekly and tumour excised on day 27. SRPK1 KD significantly reduced tumour growth ($P<0.05$, $^*P<0.01$, $^{**}P<0.001$, two-way ANOVA with repeated measures). Images of excised tumours at day 27 are shown below the graph. Scale bar, 1 cm. (**E**) RNA was extracted from tumour tissue, reverse transcribed and subjected to qPCR using SRPK1 primers and housekeeping gene (18S). SRPK1 levels were expressed as fold increase relative to the smallest tumour and correlated with tumour volume. SRPK1 expression positively correlated with tumour growth, $r=0.84$ (Pearson's correlation co-efficient). (**F**) Protein from extracted tissue was assessed for VEGF expression by ELISA. SRPK1 KD tumours expressed reduced panVEGF compared with controls. Although $VEGF_{xxx}b$ expression was unchanged, tubulin confirmed equal loading.

in knockdown tumours, showing the lentiviral knockdown remained active *in vivo* and SRPK1 expression positively correlated with tumour growth. In addition, panVEGF expression was down-regulated in knockdown (KD) compared with control tumours (Ctrl), whereas $VEGF_{xxx}b$ remained unchanged (Figure 4D). This suggests SRPK1 knockdown selectively reduces the expression of pro-angiogenic $VEGF_{xxx}$ isoforms but does not affect the expression of anti-angiogenic VEGF, which could prove to be less damaging than total VEGF blockade. Previous studies have shown $VEGF_{xxx}b$ is both cytoprotective (Magnussen *et al*, 2010) and neuroprotective (Beazley-Long *et al*, 2013), and thus maintaining its expression may prove beneficial.

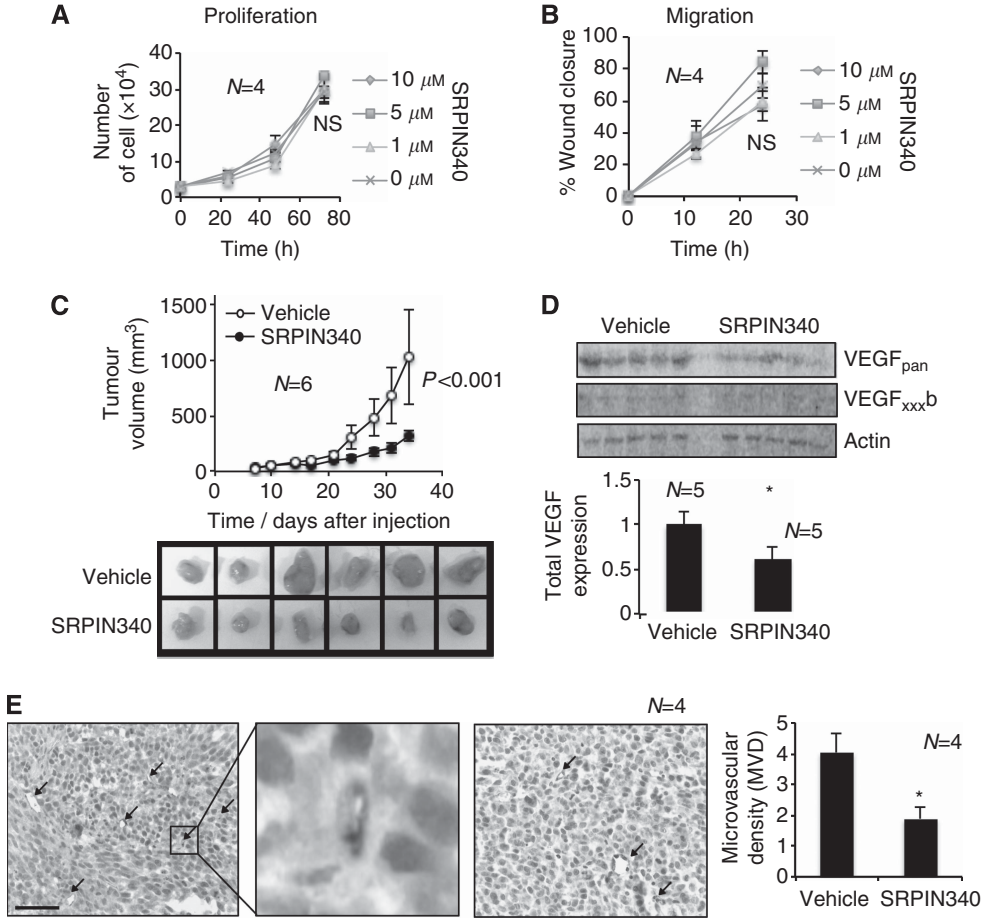

Figure 5. Small molecular weight inhibitors of SRPK1 inhibit melanoma growth. (**A**) A375 cells were treated with varying doses of SRPIN340 (1–10 μM). Cells were counted every 24 h for 3 days. There was no difference in proliferation rate between the treatments. (**B**) Wells were imaged at time 0 after a 1-mm scratch was performed across the centre of the well, and at 12 and 24 h later. The % coverage of the scratch was calculated. No statistical difference between the coverage of the cells was observed with treatment. (**C**) A375 cells were injected subcutaneously (2×10^6) in nude mice. Mice were injected subcutaneously (100 μl) with 2 μg SRPIN340 or 1% DMSO vehicle control daily. Tumour growth was measured bi-weekly and tumour excised on day 27. SRPIN340 significantly reduced tumour growth ($P<0.001$, one-way ANOVA Bonferroni *post hoc*). Images of excised tumours at day 35 are shown. Scale bar, 1 cm. (**D**) Protein from extracted tissue was assessed for VEGF expression. SRPIN340 treatment reduced panVEGF compared with control. (*$P<0.05$, unpaired t-test) $VEGF_{xxx}b$ expression was detected at very low levels but unchanged following treatment. Probing for actin confirmed equal loading. (**E**) Tumours were sectioned stained for CD31 (brown) and counterstained with haematoxylin (blue). SRPIN340 significantly reduced MVD as determined by CD31 staining compared with vehicle-treated tumours ($P<0.05$, Student's unpaired *t*-test). Scale bar, 50 μm. NS, not significant.

SRPIN340, a small molecular inhibitor targeting SRPK1, also significantly reduced tumour growth *in vivo* when injected peritumorally. Owing to a combination of low potency (μM range) and poor pharmacokinetics (Supplementary Figure 1), we were unable to successfully use this compound for systemic administration. Like SRPK1 knockdown, SRPIN340 had no effect on A375 cell proliferation or migration and resulted in reduced panVEGF expression, but not $VEGF_{xxx}b$ in treated tumours. Moreover, SRPIN340-treated tumours (unlike SRPK1 knockdown tumours) were of sufficient size to also investigate MVD. SRPIN340 treatment significantly reduced MVD compared with control confirming a mechanistic link between SRPK1 inhibition, regulating VEGF expression and angiogenesis *in vivo*.

The data presented within this study highlight SRPK1 as a potential target for the inhibition of melanoma tumour growth *in vivo*. SRPK1 inhibition acts mechanistically, at least in part, to reduce $VEGF_{165}$ expression and prevent tumour angiogenesis. It also suggests that SRPK inhibitors, such as SRPIN340 or the recently described SPHINX compounds (Gammons *et al*, 2013) may be starting points for the development of potential therapeutic agents for melanoma and pigmented cell tumours. SRPIN340 itself neither has the potency nor the pharmacokinetics to be a lead compound for drug development, but more potent, systemically active analogues of SPHINX may be next-generation anti-melanoma agents. Further investigation is also needed to elucidate other mechanisms through which SRPK1 could be acting in melanoma.

ACKNOWLEDGEMENTS

This work was supported by grants from the Skin Cancer Research Fund, the Richard Bright VEGF Research, the British Heart Foundation (PG11/20/28792), MRC grant numbers G10002073, MR/K020366/1, MR/K013157/1 and BBSRC BB/J007293/1. The authors would like to thank Dr Martine Jager, Leiden, for the provision of the uveal melanoma cell lines.

REFERENCES

Amin EM, Oltean S, Hua J, Gammons MV, Hamdollah-Zadeh M, Welsh GI, Cheung MK, Ni L, Kase S, Rennel ES, Symonds KE, Nowak DG, Royer-Pokora B, Saleem MA, Hagiwara M, Schumacher VA, Harper SJ, Hinton DR, Bates DO, Ladomery MR (2011) WT1 mutants reveal SRPK1

to be a downstream angiogenesis target by altering VEGF splicing. *Cancer Cell* **20**(6): 768–780.

Bates DO, Mavrou A, Qiu Y, Carter JG, Hamdollah-Zadeh M, Barratt S, Gammons MV, Millar AB, Salmon AH, Oltean S, Harper SJ (2013) Detection of VEGF-Axxxb isoforms in human tissues. *PLoS One* **8**(7): e68399.

Beazley-Long N, Hua J, Jehle T, Hulse RP, Dersch R, Lehrling C, Bevan H, Qiu Y, Lagreze WA, Wynick D, Churchill AJ, Kehoe P, Harper SJ, Bates DO, Donaldson LF (2013) VEGF-A165b is an endogenous neuroprotective splice isoform of vascular endothelial growth factor A *in vivo* and *in vitro*. *Am J Pathol* **183**(3): 918–929.

Bedikian AY, Millward M, Pehamberger H, Conry R, Gore M, Trefzer U, Pavlick AC, DeConti R, Hersh EM, Hersey P, Kirkwood JM, Haluska FG (2006) Bcl-2 antisense (oblimersen sodium) plus dacarbazine in patients with advanced melanoma: the Oblimersen Melanoma Study Group. *J Clin Oncol* **24**(29): 4738–4745.

Boyd SR, Tan D, Bunce C, Gittos A, Neale MH, Hungerford JL, Charnock-Jones S, Cree IA (2002) Vascular endothelial growth factor is elevated in ocular fluids of eyes harbouring uveal melanoma: identification of a potential therapeutic window. *Br J Ophthalmol* **86**(4): 448–452.

Chang AE, Karnell LH, Menck HR (1998) The National Cancer Data Base report on cutaneous and noncutaneous melanoma: a summary of 84,836 cases from the past decade. The American College of Surgeons Commission on Cancer and the American Cancer Society. *Cancer* **83**(8): 1664–1678.

Chapman PB, Hauschild A, Robert C, Haanen JB, Ascierto P, Larkin J, Dummer R, Garbe C, Testori A, Maio M, Hogg D, Lorigan P, Lebbe C, Jouary T, Schadendorf D, Ribas A, O'Day SJ, Sosman JA, Kirkwood JM, Eggermont AM, Dreno B, Nolop K, Li J, Nelson B, Hou J, Lee RJ, Flaherty KT, McArthur GA (2011) Improved survival with vemurafenib in melanoma with BRAF V600E mutation. *N Engl J Med* **364**(26): 2507–2516.

Curtin JA, Fridlyand J, Kageshita T, Patel HN, Busam KJ, Kutzner H, Cho KH, Aiba S, Brocker EB, LeBoit PE, Pinkel D, Bastian BC (2005) Distinct sets of genetic alterations in melanoma. *N Engl J Med* **353**(20): 2135–2147.

Damato B (2012) Progress in the management of patients with uveal melanoma. The 2012 Ashton Lecture. *Eye (Lond)* **26**(9): 1157–1172.

Damato B, Eleuteri A, Taktak AF, Coupland SE (2011) Estimating prognosis for survival after treatment of choroidal melanoma. *Prog Retin Eye Res* **30**(5): 285–295.

Das S, Anczukow O, Akerman M, Krainer AR (2012) Oncogenic splicing factor SRSF1 is a critical transcriptional target of MYC. *Cell Rep* **1**(2): 110–117.

Davies H, Bignell GR, Cox C, Stephens P, Edkins S, Clegg S, Teague J, Woffendin H, Garnett MJ, Bottomley W, Davis N, Dicks E, Ewing R, Floyd Y, Gray K, Hall S, Hawes R, Hughes J, Kosmidou V, Menzies A, Mould C, Parker A, Stevens C, Watt S, Hooper S, Wilson R, Jayatilake H, Gusterson BA, Cooper C, Shipley J, Hargrave D, Pritchard-Jones K, Maitland N, Chenevix-Trench G, Riggins GJ, Bigner DD, Palmieri G, Cossu A, Flanagan A, Nicholson A, Ho JW, Leung SY, Yuen ST, Weber BL, Seigler HF, Darrow TL, Paterson H, Marais R, Marshall CJ, Wooster R, Stratton MR, Futreal PA (2002) Mutations of the BRAF gene in human cancer. *Nature* **417**(6892): 949–954.

Erhard H, Rietveld FJ, van Altena MC, Brocker EB, Ruiter DJ, de Waal RM (1997) Transition of horizontal to vertical growth phase melanoma is accompanied by induction of vascular endothelial growth factor expression and angiogenesis. *Melanoma Res* **7**(Suppl 2): S19–S26.

Finetti P, Cervera N, Charafe-Jauffret E, Chabannon C, Charpin C, Chaffanet M, Jacquemier J, Viens P, Birnbaum D, Bertucci F (2008) Sixteen-kinase gene expression identifies luminal breast cancers with poor prognosis. *Cancer Res* **68**(3): 767–776.

Flaherty KT, Yasothan U, Kirkpatrick P (2011) Vemurafenib. *Nat Rev Drug Discov* **10**(11): 811–812.

Folkman J (1971) Tumor angiogenesis: therapeutic implications. *N Engl J Med* **285**(21): 1182–1186.

Gammons MV, Fedorov O, Ivison D, Du C, Clark T, Hopkins C, Hagiwara M, Dick AD, Cox R, Harper SJ, Hancox JC, Knapp S, Bates DO (2013) Topical antiangiogenic SRPK1 inhibitors reduce choroidal neovascularization in rodent models of exudative AMD. *Invest Ophthalmol Vis Sci* **54**(9): 6052–6062.

Ghosh G, Adams JA (2011) Phosphorylation mechanism and structure of serine-arginine protein kinases. *FEBS J* **278**(4): 587–597.

Gout S, Brambilla E, Boudria A, Drissi R, Lantuejoul S, Gazzeri S, Eymin B (2012) Abnormal expression of the pre-mRNA splicing regulators SRSF1, SRSF2, SRPK1 and SRPK2 in non small cell lung carcinoma. *PLoS One* **7**(10): e46539.

Gray-Schopfer V, Wellbrock C, Marais R (2007) Melanoma biology and new targeted therapy. *Nature* **445**(7130): 851–857.

Hanahan D, Weinberg RA (2000) The hallmarks of cancer. *Cell* **100**(1): 57–70.

Harper SJ, Bates DO (2008) VEGF-A splicing: the key to anti-angiogenic therapeutics? *Nat Rev Cancer* **8**(11): 880–887.

Hayes GM, Carrigan PE, Beck AM, Miller LJ (2006) Targeting the RNA splicing machinery as a novel treatment strategy for pancreatic carcinoma. *Cancer Res* **66**(7): 3819–3827.

Hayes GM, Carrigan PE, Miller LJ (2007) Serine-arginine protein kinase 1 overexpression is associated with tumorigenic imbalance in mitogen-activated protein kinase pathways in breast, colonic, and pancreatic carcinomas. *Cancer Res* **67**(5): 2072–2080.

Jemal A, Siegel R, Ward E, Hao Y, Xu J, Murray T, Thun MJ (2008) Cancer statistics, 2008. *CA Cancer J Clin* **58**(2): 71–96.

Karni R, de Stanchina E, Lowe SW, Sinha R, Mu D, Krainer AR (2007) The gene encoding the splicing factor SF2/ASF is a proto-oncogene. *Nat Struct Mol Biol* **14**(3): 185–193.

Li X, Wang J, Manley JL (2005) Loss of splicing factor ASF/SF2 induces G2 cell cycle arrest and apoptosis, but inhibits internucleosomal DNA fragmentation. *Genes Dev* **19**(22): 2705–2714.

Lipson EJ, Drake CG (2011) Ipilimumab: an anti-CTLA-4 antibody for metastatic melanoma. *Clin Cancer Res* **17**(22): 6958–6962.

Magnussen AL, Rennel ES, Hua J, Bevan HS, Beazley Long N, Lehrling C, Gammons M, Floege J, Harper SJ, Agostini HT, Bates DO, Churchill AJ (2010) VEGF-A165b is cytoprotective and antiangiogenic in the retina. *Invest Ophthalmol Vis Sci* **51**(8): 4273–4281.

Nowak DG, Amin EM, Rennel ES, Hoareau-Aveilla C, Gammons M, Damodoran G, Hagiwara M, Harper SJ, Woolard J, Ladomery MR, Bates DO (2010) Regulation of vascular endothelial growth factor (VEGF) splicing from pro-angiogenic to anti-angiogenic isoforms: a novel therapeutic strategy for angiogenesis. *J Biol Chem* **285**(8): 5532–5540.

Pritchard-Jones RO, Dunn DB, Qiu Y, Varey AH, Orlando A, Rigby H, Harper SJ, Bates DO (2007) Expression of VEGF(xxx)b, the inhibitory isoforms of VEGF, in malignant melanoma. *Br J Cancer* **97**(2): 223–230.

Stefanou D, Batistatou A, Zioga A, Arkoumani E, Papachristou DJ, Agnantis NJ (2004) Immunohistochemical expression of vascular endothelial growth factor (VEGF) and C-KIT in cutaneous melanocytic lesions. *Int J Surg Pathol* **12**(2): 133–138.

Sun S, Zhang Z, Sinha R, Karni R, Krainer AR (2010) SF2/ASF autoregulation involves multiple layers of post-transcriptional and translational control. *Nat Struct Mol Biol* **17**(3): 306–312.

Thorsen K, Mansilla F, Schepeler T, Oster B, Rasmussen MH, Dyrskjot L, Karni R, Akerman M, Krainer AR, Laurberg S, Andersen CL, Orntoft TF (2011) Alternative splicing of SLC39A14 in colorectal cancer is regulated by the Wnt pathway. *Mol Cell Proteomics* **10**(1): M110 002998.

Varker KA, Biber JE, Kefauver C, Jensen R, Lehman A, Young D, Wu H, Lesinski GB, Kendra K, Chen HX, Walker MJ, Carson 3rd WE (2007) A randomized phase 2 trial of bevacizumab with or without daily low-dose interferon alfa-2b in metastatic malignant melanoma. *Ann Surg Oncol* **14**(8): 2367–2376.

Wu Q, Chang Y, Zhang L, Zhang Y, Tian T, Feng G, Zhou S, Zheng Q, Han F, Huang F (2013) SRPK1 dissimilarly impacts on the growth, metastasis, chemosensitivity and angiogenesis of glioma in normoxic and hypoxic conditions. *J Cancer* **4**(9): 727–735.

Yang H, Jager MJ, Grossniklaus HE (2010) Bevacizumab suppression of establishment of micrometastases in experimental ocular melanoma. *Invest Ophthalmol Vis Sci* **51**(6): 2835–2842.

Zhou Z, Qiu J, Liu W, Zhou Y, Plocinik RM, Li H, Hu Q, Ghosh G, Adams JA, Rosenfeld MG, Fu XD (2012) The Akt-SRPK-SR axis constitutes a major pathway in transducing EGF signaling to regulate alternative splicing in the nucleus. *Mol Cell* **47**(3): 422–433.

Supplementary Information accompanies this paper on British Journal of Cancer website (http://www.nature.com/bjc)